

AN EXTRAORDINARY EMISSION-LINE NEBULOSITY ASSOCIATED WITH THE SEYFERT GALAXY MARKARIAN 335

TIMOTHY M. HECKMAN¹

Steward Observatory

BRUCE BALICK¹

Department of Astronomy, University of Washington

Received 1980 September 30; accepted 1981 January 16

ABSTRACT

We report the probable detection of the first known, spatially extended, broad emission-line region associated with an active galaxy or quasar. The data consist of two series of interference filter images tuned to redshifted H α and [O III] λ 5007 respectively, with each series spanning a wavelength range of ~ 200 Å (velocity range $\sim 10^4$ km s⁻¹). The extended (14" \sim 7 kpc) emission-line nebula, located $\sim 10''$ (5 kpc) from the nucleus of the type I Seyfert Mrk 335, exhibits systematic changes in strength, position, and morphology when viewed through the different filters.

A nonkinematical interpretation of the data requires the ad hoc invocation of emission lines near H α which are vanishingly weak in known astrophysical contexts. Furthermore, the fact that similar patterns can be seen in the changing position of the nebula in each of the two series of images would require the "anomalous" emission lines longward and shortward of both H α and [O III] to change their relative intensities in a coordinated fashion across the nebula.

The kinematical interpretation of the data is much less contrived and implies that gas emitting in the light of H α (plus [N II] λ 6584?) and [O III] λ 5007 is moving at 10^4 km s⁻¹ with a certain degree of order. The basic properties of the nebula are then: kinematic age $\sim 10^6$ years, temperature $\sim 10^4$ K, mass $\sim 2 \times 10^8 n_e^{-1} M_\odot$, kinetic energy $\sim 2 \times 10^{58} n_e^{-1}$ ergs. Only weak observational constraints can be placed on n_e . But, with some plausible assumptions and a simple model of nuclear ejection for the nebula, we find n_e is likely to be $\sim 10^2$ cm⁻³ and that the emitting gas is confined by the ram pressure of the halo gas in Mrk 335.

Other unusual broad-line and narrow-line knots and filaments are tentatively detected; their distribution does not appear to be highly organized. The implications of these objects are briefly discussed.

An extended, symmetric, continuum-emitting structure is also detected around the nucleus. This structure can be interpreted most plausibly in terms of its size, morphology, absolute magnitude, and possibly its color as an underlying elliptical or early-type spiral galaxy.

Subject headings: galaxies: individual — galaxies: internal motions — galaxies: nuclei — galaxies: Seyfert

I. INTRODUCTION

Much recent observational effort has shown that there is strong, albeit indirect, support for a model of active galactic nuclei of "type 1" (cf. Weedman 1977) in which a small (and from the ground, spatially unresolved) broad-line region (BLR) with dimensions ~ 0.1 pc is surrounded by a much larger, narrow-line region (NLR) with dimensions of 100 pc or more (Osterbrock 1979; Baldwin *et al.* 1980; Ulrich and Péquignot 1980; Balick and Heckman 1979, and in preparation; de Bruyn, private communication). The BLR is typified by line widths on the order of 10^4 km s⁻¹ and is apparently energized by a compact source of nonstellar radiation located at the heart of the nucleus. In every type 1 nucleus studied so far,

the BLR is both spatially unresolved and coincident with the optical/radio/X-ray nucleus of the underlying galaxy.

We report here the detection of what we believe to be a very noteworthy exception, an extended BLR associated with but clearly displaced from the nucleus (itself a Seyfert nucleus of type 1, or Sy 1) of Mrk 335. From images of Mrk 335 taken through a series of tuned narrow-band filters in the lines of H α (and [N II]) and [O III] λ 5007 (and H β), we find the extended BLR to have dimensions of ~ 7 kpc ($H_0 = 75$ km s⁻¹ Mpc⁻¹) and a projected separation from the nucleus ~ 5 kpc. Nonkinematical interpretation of the data meets with serious difficulty since it requires several ad hoc assumptions and coincidental occurrences. Interpreted more simply in kinematic terms, we find that motions in the gas are not completely random and span a range of velocities $\sim 10^4$ km s⁻¹. This extended nebular region is described in § III, and its origin and excitation are discussed in § IV.

¹ Visiting Astronomer at the Kitt Peak National Observatory, operated under contract with the National Science Foundation by the Association of Universities for Research in Astronomy, Inc.

In most other respects, Mrk 335 (1950 R.A. 00^h03^m45^s, decl. 19°55'5, $cz = 7500 \text{ km s}^{-1}$) is a very ordinary Sy 1 nucleus (a spectrum is shown in Phillips 1977). Hitherto, the only outstanding characteristic of the active system was, ironically, the apparent absence of an associated underlying galaxy. Despite the modest redshift of Mrk 335, Adams (1977) was unable to detect much more than some weak, extended fuzz to the S and E of its nucleus (see his note added in proof). From an observational standpoint, Mrk 335 is better described as an ultralow-redshift quasar of moderate luminosity $L_{\text{bol}} \sim 10^{45} \text{ ergs s}^{-1}$ (Rieke 1978; de Bruyn and Sargent 1978; Dower *et al.* 1980) than as a Seyfert "galaxy." (A second, X-ray-emitting, active nucleus of similar morphology is the QSO 0351+026, recently discovered by Margon, Chanon, and Romanishin 1981, for which $cz \sim 11,000 \text{ km s}^{-1}$.) The demonstration that the nuclei of Sy 1 galaxies and broad-line galaxies are spectroscopically indistinguishable from quasars is a linchpin in the argument that quasars are the luminous active nuclei of distant galaxies. Thus, Mrk 335 is of interest from another perspective, especially if no galaxy can be found to surround it. We report here new data which show, in fact, that the nucleus is probably located in a small-to-medium-sized, early-type galaxy of more-or-less normal color and morphology.

II. OBSERVATIONS AND DATA REDUCTION

The Kitt Peak ISIT Vidicon Video Camera was used on the 4 m Mayall telescope (Robinson *et al.* 1979) for the present observations. The Video Camera format is a 256×256 pixel array which at the Ritchey-Chrétien focus of the 4 m telescope has a scale of 0".292 per pixel or a field of view of $\sim 70'' \times 70''$ after correction for spatial distortion in the instrument. The observations consist of one image obtained through a V filter and 10 images obtained through nearly square bandpass interference filters (FWHM $\sim 55\text{--}75 \text{ \AA}$) with responses centered at wavelengths corresponding to velocities cz from 1000 to

10,000 km s^{-1} in 3000 km s^{-1} increments for [O III] $\lambda 5007$, and 2000 to 12,000 km s^{-1} in 2000 km s^{-1} increments for H α (Table 1). Integration times were 13 minutes per image. The nuclear image is saturated only in the V image and in the two H α images nearest the wavelength of the nuclear H α line.

To provide an absolute flux calibration for our observations, we observed the standard stars EG 31 = HZ 2 through each of the H α interference filters and EG 29 = LB 227 (Oke 1974) through each of the [O III] filters. All of the data were calibrated and reduced in the standard way by using observations of a quartz lamp to correct for pixel-to-pixel variations in the detector sensitivity and observations of a uniformly illuminated twilight sky to correct for low-spatial-frequency sensitivity variations. Corrections for spatial distortion in the images were made using the standard parameters available at Kitt Peak. No ghosts, knots, or internal reflections are seen in the images of the standard stars.

The data were all obtained during a 3-hour period in 1979 November under excellent and stable observing conditions. We measured the image profile widths of the standard stars (the "seeing") to be ~ 1.3 FWHM throughout the observations. The quality of the data thus allows us to fit a seeing profile to the nucleus of Mrk 335 and to subtract it digitally from each nonsaturated image. This fit was made using the sum of the observations of the standard stars to define the seeing profile. (The profile was found to match the image of a faint star located $\sim 20''$ SW of the nucleus out to a radius of $\sim 3''$.) Subtraction of the short-integration, stellar, seeing profile necessarily degrades the signal-to-noise in the deeper Mrk 335 images, so these images with the bright nucleus of Mrk 335 suppressed were used only to search for a faint underlying galaxy.

We show photographic representations of the four original [O III] images (Fig. 1), the six H α images (Fig. 2), and the sum of the [O III] images, the sum of the H α images, the sum of the [O III] and H α images, and the V image (Fig. 3). Two transfer functions determining con-

TABLE 1
FILTER CHARACTERISTICS AND LINE FLUXES

Emission Line (\AA)	Center (\AA)	Velocity (km s^{-1})	Width (\AA) ^a (FWHM)	Relative Transmissivity ^b	Flux ($10^{-15} \text{ ergs cm}^{-2} \text{ s}^{-1}$)
...	5025	1000	55	$\equiv 1.00$	10.2
...	5075	4000	56	1.05	6.8
[O III] ^c	5125	7000	54	1.12	10.8
$\lambda 5007$	5175	10000	58	1.04	3.4
...	6607	2000	76	$\equiv 1.00$	5.3
...	6650	4000	69	0.86	9.3
H α ^d	6694	6000	72	0.91	27.2
$\lambda 6563$	6738	8000	76	0.96	21.9
...	6782	10000	75	0.92	10.9
...	6826	12000	74	0.95	2.4

^a All filter widths correspond to about 3300 km s^{-1} in the associated emission lines.

^b Measured for continuous spectrum.

^c [O III] $\lambda 4959$ velocity = [O III] $\lambda 5007$ velocity + 2900 km s^{-1} . H β velocity = [O III] $\lambda 5007$ velocity + 8700 km s^{-1} .

^d [N II] $\lambda 6584$ velocity = H α velocity - 1000 km s^{-1} .

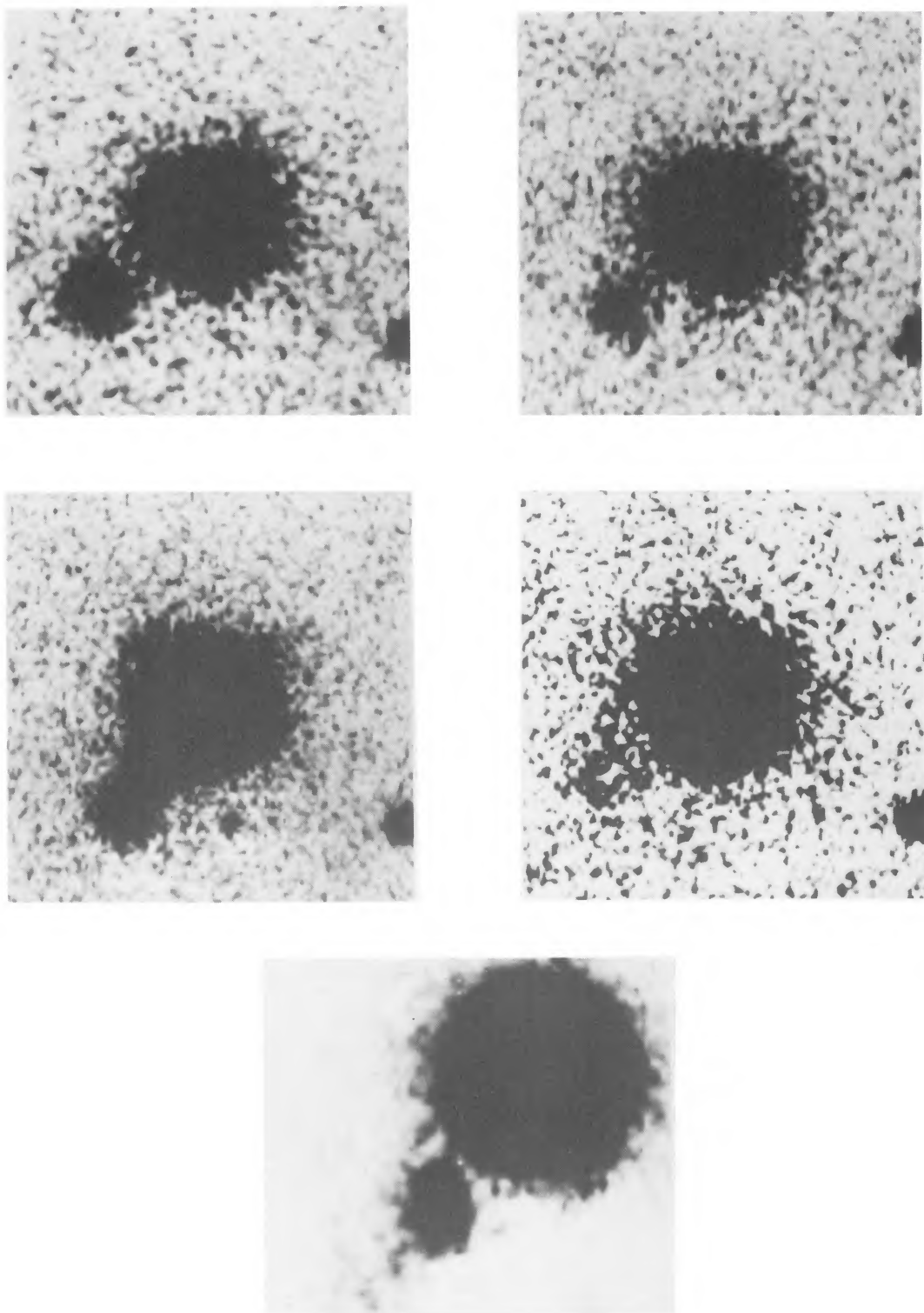


FIG. 1.—Photographic representations of the four Mrk 335 images obtained through the $[O\ III]\ \lambda 5007$ interference filters, arranged from left to right and then top to bottom, in the order $\lambda 5025$, $\lambda 5075$, $\lambda 5125$, and $\lambda 5175$. North is to the top, and East is to the left, with the size of the field represented being $37''.4$. Below is a low-contrast enlargement of a $17''.2$ field of the $\lambda 5125$ frame which shows Knot 1.

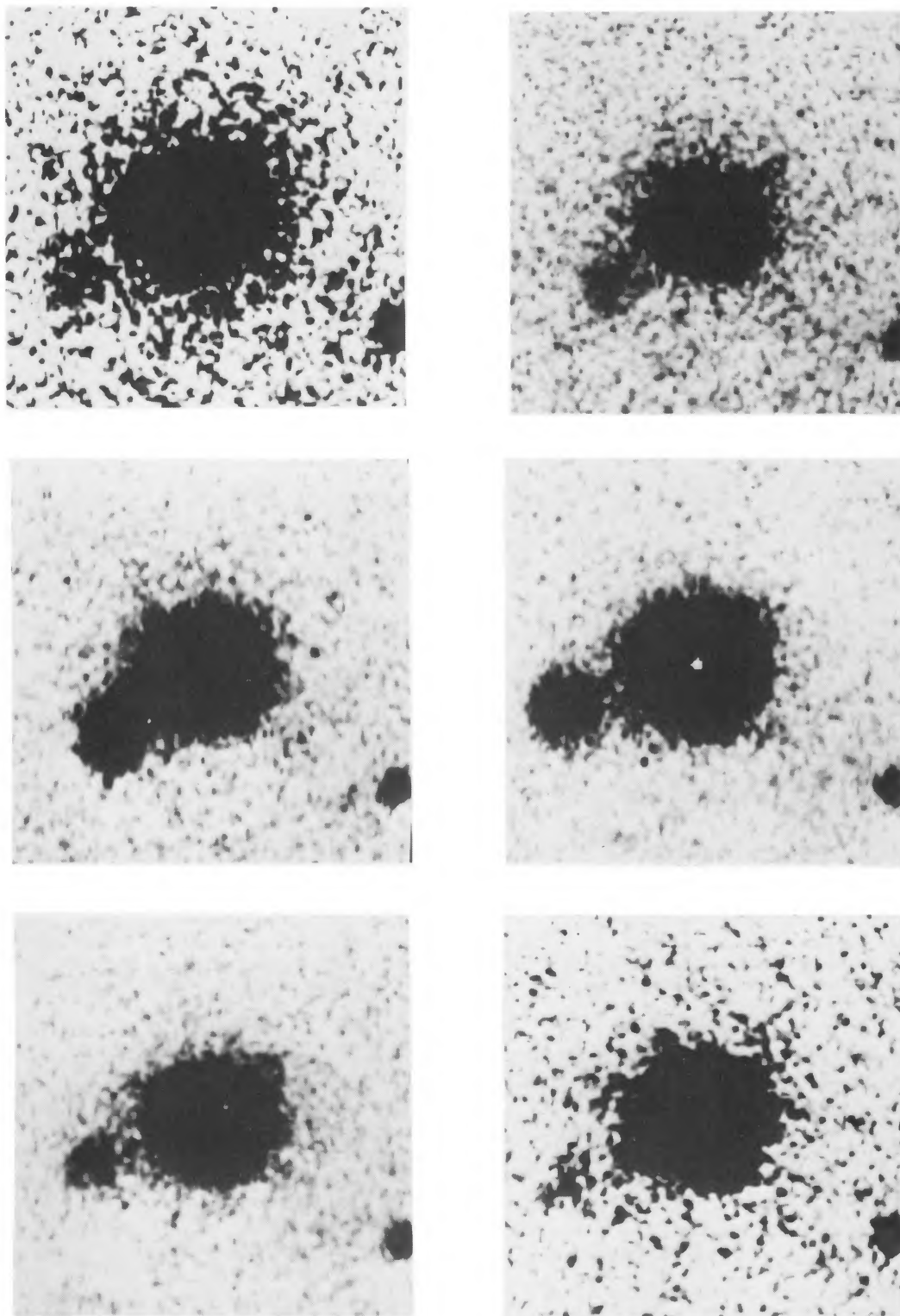


FIG. 2.—Photographic representation of the six Mrk 335 images obtained through the $H\alpha$ interference filters, arranged from left to right and then top to bottom, in the order $\lambda 6607$, $\lambda 6650$, $\lambda 6694$, $\lambda 6738$, $\lambda 6782$, and $\lambda 6826$. Scale and orientation are as given in Fig. 1.

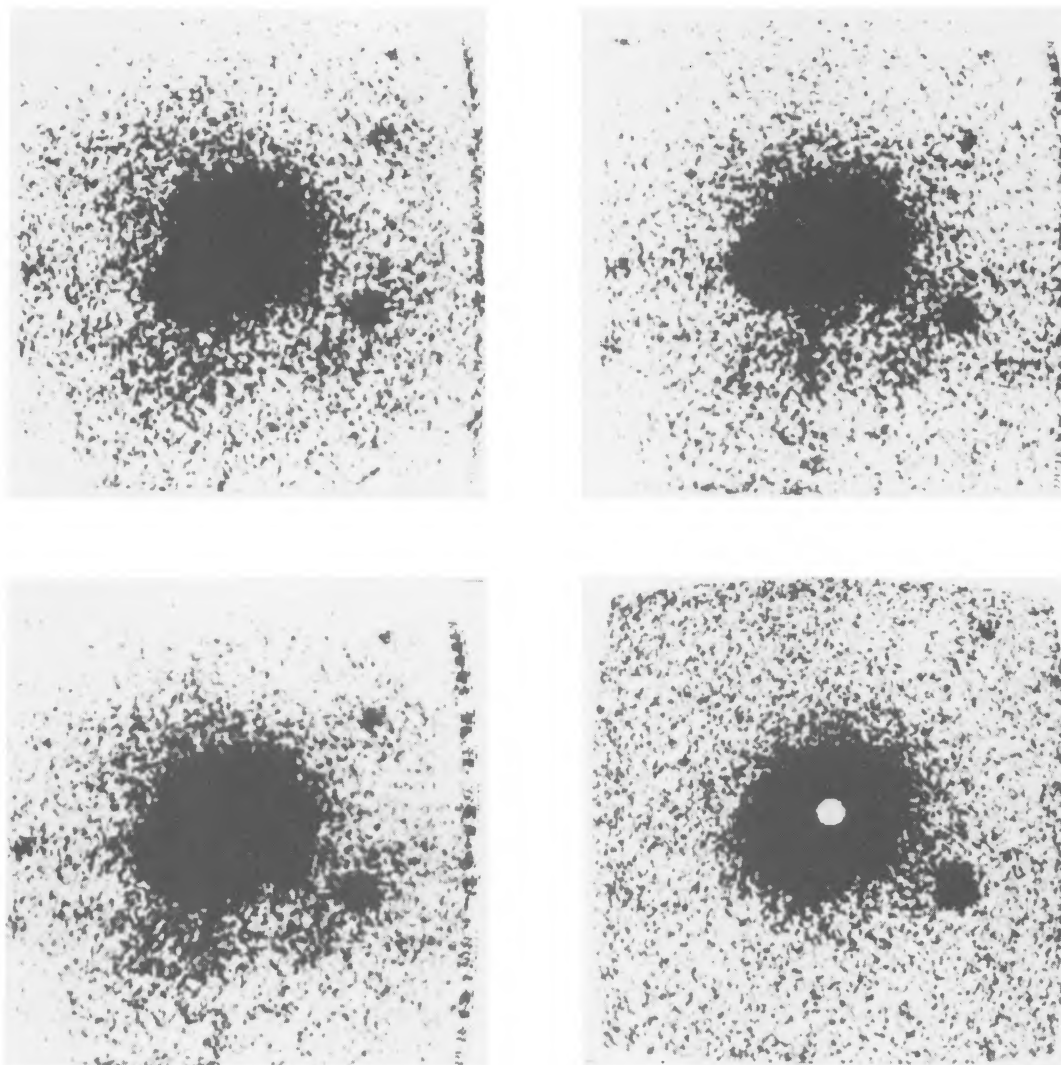


FIG. 3.—Photographic representation of (from left to right and then top to bottom) the sum of the four [O III] $\lambda 5007$ images, the sum of the six H α images, the sum of the 10 [O III] and H α images, and the V image. North is to the top, east is to the left, and the imaged field is $74'' \times 8''$. The position of the nucleus can be located (only) in the V image owing to a digital overflow; note that the nucleus is NE of the center of the black area in these prints which are extremely high in contrast.

trast and brightness were used to display the images in Figures 1 and 2, with the higher contrast one used for the relatively low signal-to-noise $\lambda 5175$, $\lambda 6607$, and $\lambda 6286$ frames. All the images in Figure 3 (the summed pictures) were displayed in the same way to facilitate comparisons of the images.

III. RESULTS

a) The “Moving Nebula”

The remarkable nature of the “moving nebula” and the origin of its name can be appreciated from an inspection of Figures 1 and 2. Table 1 gives the velocity appropriate to redshifted [O III] $\lambda 5007$ and H α for each filter in the two respective series and summarizes the changes in the strength of the nebula in the different

images. Figure 4 summarizes the changes of the position angle of the centroid of the nebula with respect to the nucleus of Mrk 335 as the filter was changed. Here, the x-axis has been labeled in units of km s^{-1} relative to the systematic velocity of the nucleus ($V_{\text{SYS}} = 7500 \text{ km s}^{-1}$) assuming the emission to be due to [O III] $\lambda 5007$ and H α in the two respective image series.² We discuss this assumption critically below. These figures and Table 1, together with the relative weakness of the nebula in the V-band image shown in Figure 3 provide ample evidence for the identification of the nebula with emission-line gas.

These are two primary ways of interpreting the results shown in Figures 1–4. The first, or “nonkinematical,”

² All velocities will henceforth be given relative to V_{SYS} unless otherwise noted.

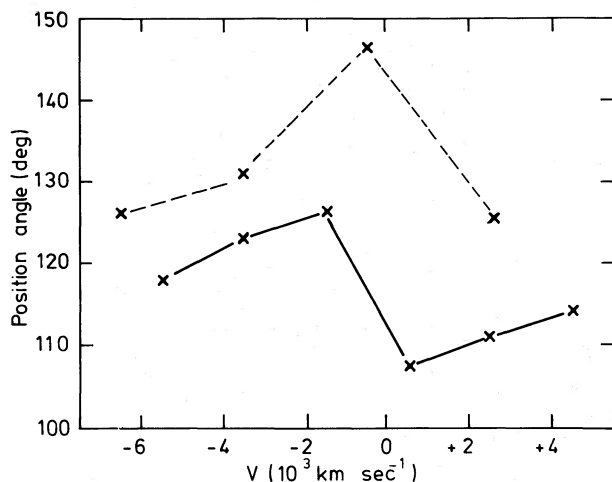


FIG. 4.—Plot of the position angle of the center of the “moving nebula” as a function of its velocity. The solid line pertains to the $H\alpha$ images and the dashed line to the $[O III]$ images. Uncertainties are of the order of $\pm 3^\circ$, except for the $H\alpha$ points at -5500 and $+4500 \text{ km s}^{-1}$ and the $[O III]$ point at $+2500 \text{ km s}^{-1}$ where the uncertainties are about $\pm 5^\circ$.

interpretation is that the changes in the appearance of the nebula in the different images is caused by *different* emission lines which are observed through the different filters. Movement of the nebula from image to image would then require systematic changes on a large spatial scale in the relative strengths of the various lines. The wavelength region around $[O III] \lambda 5007$ is, in fact, somewhat confused in the spectra of many Seyfert galaxy nuclei with $H\beta$, $[O III] \lambda 4959$, and the Fe II complex of lines all present. However, the region around $H\alpha$ is far more “clean,” since $[N II] \lambda 6548$ and $[N II] \lambda 6584$ are the only other lines which are commonly strong in the wavelength region of interest. In fact, the offset in wavelength between the $H\alpha$ and $[N II]$ lines is far smaller than the wavelength range spanned by the images in Figure 2. (It is even smaller than the spectral resolution of the filters, so that $[N II]$ emission will not seriously complicate interpretation of the images in terms of $H\alpha$ emission.) To explain the wide wavelength range around $H\alpha$ over which emission is observed, one can always turn to an extensive table of atomic transitions and then invoke *some* set of lines which are vanishingly weak in known astrophysical contexts. (Such an approach was tried in early attempts to explain the spectra of “quasi-stellar radio sources” in terms of galactic stars at zero redshift.)

In addition to the rather ad hoc nature of such a model, it has several specific difficulties with the data. The first is that Table 1 shows the nebula’s integrated flux to be quite symmetrical about the wavelength of the nuclear $H\alpha$ line. An explanation in terms of a “zoo” of anomalous emission lines would require the relative strengths of these lines to be fortuitously dependent upon their wavelength with respect to $H\alpha$. While the flux from the nebula in the $[O III]$ image series does not show the same symmetry, this is presumably due to confusion with $H\beta$ and $[O III] \lambda 4959$ as described above.

Another problem with the nonkinematical model can be seen in Figure 4, in which it is clear that both series of images show similar patterns in the change of the position of the nebula with wavelength. A dramatic, clockwise change in position occurs in the $H\alpha$ ($[O III]$) image series close to the wavelength of the nuclear $H\alpha$ ($[O III] \lambda 5007$) line. A further systematic, though less pronounced, change can also be seen in *both* series of images: as the wavelength of the emitting gas increases, the nebula appears to move in a counter-clockwise direction, until the rather abrupt, clockwise “jump” described above. In the nonkinematical interpretation, a highly fortuitous and unlikely set of circumstances must be invoked to explain these phenomena. One must assume that the lines shortward of $H\alpha$ are relatively strong in the same portion of the nebula as the *a priori* unrelated lines shortward of $[O III] \lambda 5007$, with the same situation applying to the lines longward.

As can be seen, the nonkinematical interpretation of the “moving nebula” is highly implausible, and for this reason we strongly favor a kinematical interpretation. Of course, the presence of $H\beta$ (effective velocity offset of -9000 km s^{-1} with respect to $[O III] \lambda 5007$), $[O III] \lambda 4959$ (offset $\sim -2900 \text{ km s}^{-1}$), and the Fe II complex will complicate interpretation of the $[O III]$ series of images. Judging from the $H\alpha$ images and assuming that $F_{H\beta}/(F_{H\alpha} + F_{[N II]}) \leq 0.35$ (i.e., \leq an unreddened case B value with $F_{[N II]} = 0$), $H\beta$ will contribute significantly only to the $\lambda 5025$ image, where as much as $\sim 30\%$ of the nebular flux could come from $H\beta$ (corresponding to the $H\alpha$ emission in the $\lambda 6782$ frame). The $[O III] \lambda 4959$ line is constrained by atomic physics to be only roughly one-third as bright as the $\lambda 5007$ line. It will then contribute in a known and relatively unimportant way to the images.

As we have argued above, interpretation of the $H\alpha$ series of images will not be complicated seriously by the presence of $[N II]$. The primary conclusions discussed below will hence be drawn from this image series, and the $[O III]$ series will be used to support these conclusions, insofar as the two image series are consistent. We will henceforth speak of “velocities” assuming that we are measuring the $H\alpha$ line and the $[O III] \lambda 5007$ line in the two respective image series. We will limit our kinematical discussion to a level in which the ambiguities discussed above are not crucial.

Interpreted kinematically, the gas in the “moving nebula” is detected through filters spanning a range from -6500 to $+4500 \text{ km s}^{-1}$ relative to V_{SYS} . However, the true velocity range of the gas could be somewhat smaller than this value, because of the finite filter bandwidths and the blending of $H\beta$ and $[O III] \lambda 4959, 5007$ and of $H\alpha$ and $[N II] \lambda 6548, 6584$, as discussed above. On the other hand, the nebula is visible in all of the images taken and could extend to more extreme velocities than we were able to observe.

As we have described previously, Figure 4 shows evidence for a systematic change in the position of the nebula as a function of velocity. But, as Figure 4 also shows, the $H\alpha$ images tend to be shifted by about $15^\circ \pm 5^\circ$ clockwise with respect to the $[O III]$ images at any given

velocity. This offset is several times too large to be accounted for by measurement uncertainties, filter overlap, or by the line-blending mentioned above even if [N II] is much stronger than H α in the nebula. We discuss the implications of this offset briefly below.

The total extent of the nebula is $\sim 14''$ (~ 7 kpc), and it is centered $\sim 10''$ (~ 5 kpc) from the nucleus. The nebula appears as a symmetric, featureless, centrally condensed "blob" in all the frames except the [O III] frame taken closest to V_{SYS} (filter $\lambda 5125$). Here, in addition to the smooth, diffuse emission, two small knots (see Fig. 5) can be seen $\sim 7''$ SSE and $\sim 11''$ SSW of the nucleus (called "Knot 1" and "Knot 2" respectively). Knot 1 accounts for $\sim 50\%$ of the flux from the nebula at this velocity and is $\sim 3 \times 2''$ in size, elongated in a position angle of 15° – 20° . Knot 2 is much fainter and appears unresolved. Since the knots have no analog in the H α images, they presumably consist of highly excited gas [$F_{[\text{O III}]} \gtrsim 1.5 (F_{\text{H}\alpha} + F_{[\text{N II}]})$]. Although the integrated ratio of $F_{[\text{O III}]}$ to $(F_{\text{H}\alpha} + F_{[\text{N II}]})$ in the rest of the nebula appears to be considerably smaller than this (~ 0.6), the systematic differences between the [O III] and H α images (Fig. 4) mean that large variations in the ratio occur in the nebula.

We find no evidence for the presence of the above knots in the $\lambda 5075$ frame. ([O III] $\lambda 4959$ emission corresponding to the [O III] $\lambda 5125$ frame should be present with roughly one-third of the $\lambda 5007$ intensity, this ratio being set by atomic physics.) In the case of Knot 2, a feature of the required strength could easily go undetected in the $\lambda 5075$ frame. However, in the case of Knot 1 one *would* expect to detect the presence of $\lambda 4959$ emission in the $\lambda 5075$ frame

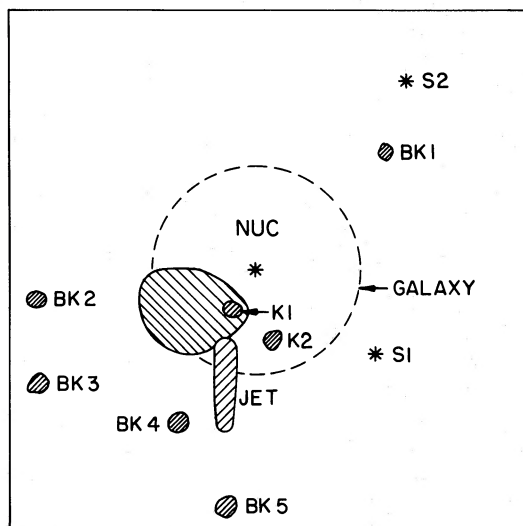


FIG. 5.—Schematic diagram showing the location of various features described in the text. "MN" indicates the "moving nebula," "K1" and "K2" are Knots 1 and 2 respectively. "Jet" refers to a possible, elongated, "broad-H α " feature, and "BK1," "BK2," "BK3," "BK4," and "BK5" refer to five possible "broad-emission-line" knots. The measurable extent of the surrounding galaxy is indicated by a dashed circle. The position of the nucleus of Mrk 335 is also indicated ("Nuc") as are the positions of two, faint, continuum-emitting objects which are presumably stars ("S1" and "S2").

even though its signal-to-noise ratio would not be high. (It is very difficult to make this statement more quantitative in view of the steep intensity gradient and correspondingly steep noise gradient across the position of Knot 1.) If it is *not* present at the proper level, Knot 1 must be an emission-line feature produced by a different emission line at a different velocity (H β at $\sim +8800$ km s^{-1} ?). Spectroscopy of Knot 1 is obviously important.

In addition to the knots and the "moving nebula," a number of faint features which are visible in the sums of the interference filter frames but not in the V image may be distinguished. Since the effective throughput of the V filter is ~ 5 , 3, and 2 times larger respectively than that of the [O III], H α , and [O III] + H α filter sums, these must then also be emission-line objects. Moreover, these features are more pronounced in the sums of the emission-line frames than in any individual frame, so they must be "broad-emission-line" features as well. (These statements are substantiated by integrations of the counts from each feature in the individual and summed frames.) The features consist of several knots which are seen most clearly in the H α + [O III] sum and an elongated feature to the S and SE of the nucleus which is most clearly seen in the H α sum (see Fig. 5). Since the implications of these features (see below) are even more extraordinary than those of the "moving nebula," it is vitally important to confirm their nature as broad-emission-line objects.

b) The Underlying Galaxy

In addition to the emission-line features discussed above, we have probably succeeded in detecting an underlying galaxy in Mrk 335. We believe that it is a galaxy because it must consist primarily of continuum-emitting material, and it has the proper size, morphology, radial surface-brightness profile, and absolute magnitude to be either a face-on, early-type spiral (Sa or S0) or an E0-E2 galaxy. More sophisticated imaging, accurate photometry, and (most importantly) spectroscopic detection of normal stellar absorption features at $cz \sim 7500$ km s^{-1} will be required before this continuum-emitting material can be identified conclusively with a galaxy of stars, rather than with something more exotic. We will continue to refer to it as a "galaxy" since that is the simplest interpretation consistent with the present observations.

The fact that the underlying galaxy emits primarily in the continuum is based on a comparison of its surface brightness in the V image to that in the sum of the unsaturated [O III] and H α images. The comparison was done in an annulus from $9''$ to $14''$ from the nucleus. At this distance, the seeing-profile of the central nucleus has dropped to a negligible level so that a subtraction of the nucleus is not necessary. (Such a subtraction was not attempted for the V image because the nucleus was heavily saturated.) No significant excess in the surface brightness in the [O III] or H α sums relative to V was observed (after a subtraction of the contribution made by the emission-line nebulosity discussed above).

The galaxy appears to be rather featureless and circularly symmetric. This suggests that, if it is a true galaxy

of stars, it is either an E0-E2 or a face-on, bulge-dominated, disk galaxy. The radial surface-brightness profile is well fitted with a simple Hubble profile, as illustrated in Figure 6. It is then most likely an elliptical galaxy. The characteristic diameter of the galaxy within which half the luminosity is emitted is $\sim 7''$ or 3.5 kpc. We estimate that the total apparent magnitude of the galaxy is $m_v \sim 15$ which implies that $M_v \sim -20$. Thus, the size and luminosity of the galaxy are quite typical of a medium-sized elliptical. The fact that it has hitherto escaped detection is a result of its circular symmetry, its small angular size, and the relatively high luminosity of the nucleus. (The galaxy accounts for only $\sim 20\%$ of the continuum luminosity of Mrk 335.)

The color of the galaxy, as best as we can estimate from the ratio of its brightness in the [O III] and H α filters, is $(V-r) \sim 0.35 \pm 0.20$. This is probably not significantly bluer than the color of a typical, early-type galaxy, $(V-r) \sim 0.50 \pm 0.10$ (Sandage and Visvanathan 1978), but more careful photometry will be required to confirm this.

IV. DISCUSSION

Fairly simple considerations lead to some interesting constraints on the Mrk 335 nebula. First, dividing the size of the emission-line nebula by a characteristic velocity implies a kinematic age of $\lesssim 10^6$ years for the moving nebula and $\lesssim 10^5$ years for the fainter knots and the jet (if the transverse dimension of the jet is used). Since we regard the nature of the jet and faint knots as still somewhat uncertain, we will use 10^6 years as the maximum age of the nebula.

From the presence of both [O III] $\lambda 5007$ and H α (plus [N II] $\lambda 6584$?), we deduce that gas at temperatures of 5000–50,000 K must be present and that this gas cannot be wholly unprocessed material (e.g., some oxygen and possibly nitrogen is present). The total H α luminosity of the moving nebula is $\sim 5 \times 10^{40}$ ergs s^{-1} which implies

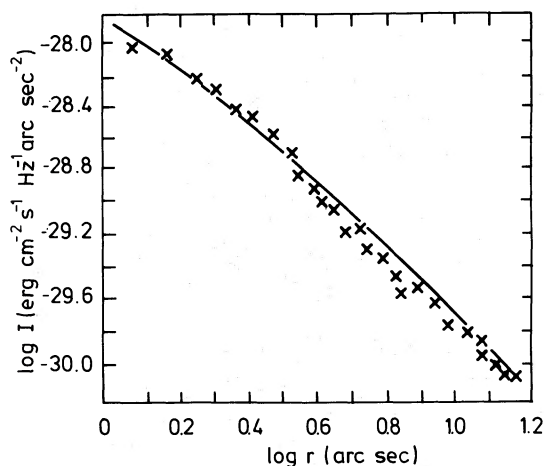


FIG. 6.—The logarithm of the surface brightness (in ergs $cm^{-2} s^{-1} Hz^{-1} arcsec^{-2}$) of the galaxy surrounding Mrk 335 plotted against the logarithm of the distance from the nucleus. The solid line shows a Hubble profile fitted to the data.

that $M_{H^+} \sim 2 \times 10^8 n_e^{-1} M_\odot$. Taking a characteristic gas velocity of $\sim 10^{3.5}$ km s^{-1} then implies a kinetic energy of $KE \sim 2 \times 10^{58} n_e^{-1}$ ergs. This can be compared with the binding energy of a typical galaxy ($\sim 10^{59}$ ergs) or the equipartition energy in relativistic particles plus magnetic field in a typical double radio source ($\sim 10^{58}$ ergs).

Estimates of n_e are unavoidably indirect and uncertain. The minimum value for n_e comes if the filling factor of the emission-line gas in the nebula is unity. Taking the nebula to be roughly spheroidal with $r \sim 3.5$ kpc then implies $n_e \geq 0.25 cm^{-3}$ so that $M_{H^+} \lesssim 10^9 M_\odot$ and $KE \lesssim 10^{59}$ ergs.

If we constrain the kinetic energy of the nebula to be equal to the luminous output of the nucleus over 10^6 years which has been directed into the ~ 1 sr covered by the nebula, we find that $KE \sim 3 \times 10^{57}$ ergs, $n_e \sim 5 cm^{-3}$, and $M_{H^+} \sim 3.5 \times 10^7 M_\odot$.

The mass, density, and energy estimates apply only to that fraction of the ionized gas at $T \sim 10^4$ K. The bulk of the mass and energy in the nebula could reside in material having very different physical conditions. Certainly, with gas velocities of thousands of km s^{-1} , one might expect a diffuse, hot medium at $\sim 10^9$ K to coexist with the cool, optically emitting clouds. Conceivably, the optical emission arises in an energetically unimportant transition zone at $T \sim 10^4$ K between hotter and cooler media or some local instability of a transient nature.

We can consider if the source of ionization of the nebula is the active nucleus. The ultraviolet luminosity of Mrk 335 can be interpolated from its infrared, optical, and X-ray fluxes (Rieke 1978; de Bruyn and Sargent 1978; Dower *et al.* 1980) as $L_{UV} \sim 10^{44}$ ergs s^{-1} (3×10^{54} photons $s^{-1} rydberg^{-1}$). The solid angle Ω of the nebula subtended at the nucleus is very uncertain, but $\Omega \sim 0.1 \times 4\pi$ seems reasonable, so that $\sim 10^{43}$ ergs s^{-1} of ionizing radiation enters the cloud. From the H α flux, it appears that only about 10% of the incident ionizing radiation is absorbed within the cloud, but the large uncertainties in Ω make it conceivable that the nebula is optically thick. Thus, an adequate ionizing continuum from the nucleus does appear to exist, although other ionizing sources may also be present.

We now wish to consider a class of models which we regard as a relatively conservative picture of the Mrk 335 phenomenon. It seems most likely that the high velocities observed in the nebula had their origin in the nucleus. It is rather striking that the velocities in the nebula are quite similar to those typical of the BLR in type 1 Seyferts and QSOs (e.g., Osterbrock 1977). We can investigate the point of view that the nebula is simply composed of ejecta from the BLR at a temperature like that in the BLR ($\sim 10^4$ K) since models in which outflow is the dominant line-broadening agent are now favored for the BLR (e.g., Ferland, Netzer, and Shields 1979; Capriotti, Foltz, and Byard 1979).

The kinematics and morphology of the moving nebula suggest that we are seeing gas which has been ejected in such a way that, near the bottom of the nebula, the gas is moving primarily tangentially to the line of sight, while, at

the top, we see some gas moving toward us at several thousand km s^{-1} and some moving away at similar velocities. In this picture, the true ejection velocity is likely to be $\sim 10^4 \text{ km s}^{-1}$ in order to give projected radial velocities of several thousand km s^{-1} . However, a detailed knowledge of the spatial geometry is not crucial to the discussion which follows.

Thus, we can calculate that gas has been ejected from the BLR for $\sim 7 \text{ kpc}/10^4 \text{ km s}^{-1} \sim 10^6$ years. The typical mass of H^+ in the BLR is $\sim 10 M_\odot$ (Osterbrock 1977). Thus, outflow of this gas from the BLR, which has $r \sim 3 \times 10^{17} \text{ cm}$ from observed emission-line variability (de Bruyn, private communication), at 10^4 km s^{-1} yields $\dot{M} \sim 1 M_\odot \text{ yr}^{-1}$. The mass of the gas in the nebula will then be $\sim 10^6 M_\odot$, requiring that $n_e \sim 200 \text{ cm}^{-3}$, or $\text{KE} \sim 10^{56}$ ergs.

Next, we consider the likelihood of nebular confinement. During a transit time of 10^6 years, a cloud expanding sonically will grow to a size of 10 pc if its temperature is 10^4 K . Were this the case then for $n_e \sim 200 \text{ cm}^{-3}$, each individual cloud mass, $\sim 2 \times 10^3 M_\odot$, would be much larger than the mass of the BLR ($\sim 10 M_\odot$) from which it was supposedly ejected. In order to make these cloud masses more reasonable, we assume that the nebula consists of numerous smaller clouds confined by some mechanism. Since the clouds are traveling at $\sim 10^4 \text{ km s}^{-1}$, ram pressure confinement by an external medium is an obvious possibility. Taking a thermal pressure inside the cloud of $nkT \sim 3 \times 10^{-10} \text{ dynes cm}^{-2}$, the ambient medium would have a required density of only $2 \times 10^{-4} \text{ cm}^{-3}$. The models of Bregman (1980) predict densities of $\sim 10^{-4} \text{ cm}^{-3}$ at $r \sim 5 \text{ kpc}$ in galactic coronae which are at $T \sim 10^6 \text{ K}$, while the gaseous halo models of Norman and Silk (1979) predict temperatures and densities about an order of magnitude larger. Thus, the cloud motions will be highly supersonic, and ram pressure should be sufficient to confine the clouds. The drag on the clouds by the halo gas will slow them down, but such a braking will only be significant for clouds having small column densities (e.g., clouds that are smaller than $r \sim 6 \times 10^{-3} \text{ pc}$ or $M_{\text{cloud}} < 10^{-5} M_\odot$).

The morphology of the nebula suggests, perhaps, that the ejection was highly anisotropic, with the clouds all being ejected into $\sim 1 \text{ sr}$ by the nucleus. Alternatively, the nuclear ejection of material may have been initially symmetric, with asymmetric extranuclear collimation taking place. Highly collimated ejection of relativistic plasma is commonly seen in radio-loud quasars and radio galaxies, and can even be one-sided (as in the D2 class of radio sources described in Miley 1980). However, the lack of observable radio lobes suggests that any collimation mechanism operative in Mrk 335 is dissimilar to the common mechanisms affecting the structure of radio galaxies. Perhaps more relevant is the discovery (M. Burbidge, private communication; Weymann, private communication) that approximately 10% of optically selected quasars show broad, detached $\text{Ly}\alpha$ and $\text{C IV } \lambda 1549$ absorption features. As Turnshek *et al.* (1980) have argued, the most straightforward interpretation of these features is that outflow which is collimated into $\sim 10\%$ of

the sky (e.g., into $\sim 1 \text{ sr}$) is occurring in high-redshift quasars. This compares quite nicely with the Mrk 335 model described above. A less exotic possibility for explaining the asymmetric morphology of the moving nebula is that it is a unique and lone survivor of clouds injected into the galactic halo. (Note that the faint, broad-emission-line knots show no strong, preferential orientation.) Or, other "moving nebulae" may exist near Mrk 335, but physical conditions in these objects (e.g., temperatures $\gg 3 \times 10^4 \text{ K}$ or low emission measures in $\text{H}\alpha$ and $[\text{O III}]$) render them difficult to detect in the present observations.

Our simple picture of the Mrk 335 nebula as ejecta from the active nucleus of the galaxy thus does not directly explain the nebula's asymmetrical structure. There are a number of other properties of the nebula that the model also does not address. First, we have shown that the $\text{H}\alpha$ and $[\text{O III}]$ emitting regions exhibit different dependencies of their position angles on velocity in the moving nebula (Fig. 4). Clearly, large-scale variations in the physical conditions within the nebula must be taking place. The $[\text{O III}] \lambda 5007$ emission might come preferentially from regions which have higher temperatures (enhanced collisional excitation of the $[\text{O III}]$ transition), proper ionization state (relatively large ratio of O^{+2}/O), or even $n_e \ll 10^7 \text{ cm}^{-3}$ (negligible collisional de-excitation of $[\text{O III}] \lambda 5007$).

The ejection picture faces difficulty in explaining the faint knots and "jet" described above if they are, as the evidence strongly suggests, broad-emission-line objects. Their dynamical lifetimes (diameter divided by velocity spread) of $\sim 10^5$ years would then be very short compared with their travel times from the nucleus ($\geq 10^6$ years for an ejection velocity $\leq 10^4 \text{ km s}^{-1}$). In situ acceleration of the gas may well be required for these objects, as is now thought to be required for the relativistic particles in the lobes of radio galaxies (Miley 1980).

Finally, our model does not address the question of why Mrk 335, alone among the 35 active galaxies we have observed (in preparation), shows this extraordinary nebula. The only other unusual property of Mrk 335 relative to other objects in our sample is the high contrast of the nucleus relative to the underlying galaxy. A careful look at morphologically similar objects (very low redshift quasars) may be enlightening in this regard.

V. SUMMARY

Extended nebulosity whose emission lines span a wavelength range of $\sim 200 \text{ \AA}$ has been observed $\sim 10''$ SE of the active nucleus of the type 1 Seyfert galaxy Mrk 335. A nonkinematical explanation of the nebula requires the ad hoc invocation of anomalous emission lines near the wavelength of $\text{H}\alpha$ which are vanishingly weak in known astrophysical situations. To explain the data, the anomalous emission-lines near $\text{H}\alpha$ and $[\text{O III}] \lambda 5007$ in wavelength must act in concord in a highly unlikely way (conclusion 2 below) and must be symmetrically located in wavelength with respect to $\text{H}\alpha$, while diminishing in strength as a function of their offset in wavelength from $\text{H}\alpha$. This situation is so highly contrived that we strongly

prefer a kinematic interpretation of the data. The salient characteristics of the nebula are then:

1. $H\alpha$ and [O III] emission at velocities (relative to the nucleus) of -6500 to $+4500$ km s^{-1} . Lines as broad as this have hitherto been reported only in the spatially unresolved nuclei of Seyfert galaxies, radio galaxies, and quasars.

2. A clear pattern of organized motions within the nebula. (The nebula appears to shift position by more than $10''$ [5 kpc] in emission-line images spanning a velocity range of 10^4 km s^{-1} .) This motion is seen in the same sense in both the $H\alpha$ and [O III] images.

3. The nebular extent is ~ 7 kpc, and the projected nuclear distance is 5 kpc.

4. The integrated nebular ionization is characterized by $F_{[\text{O III}]} \sim 0.6 (F_{H\alpha} + F_{[\text{N III}]})$, but there is apparent positional offset of the $H\alpha$ and [O III] images by ~ 3 kpc.

5. There is apparent absence of a counterpart on the opposite side of the galaxy (or elsewhere within the $70''$ field of view).

Small knots of broad line emission also are seemingly present in the vicinity of Mrk 335, but little is known about their morphology. The distribution of knots in the field appears to be almost random, although a preference for the SE and NW quadrants of the field can be noted.

When the seeing-disk of the nucleus of Mrk 335 is removed, the presence of continuum-emitting material, whose characteristics are consistent with those of a normal, medium-sized elliptical galaxy (or nuclear bulge) is detected.

From the observational data alone, we estimate a mass $M_{H^+} \sim 2 \times 10^8 n_e^{-1} M_\odot$, kinetic energy $2 \times 10^{58} n_e^{-1}$ ergs for the nebulosity, and from elementary considerations $n_e \geq 0.25 \text{ cm}^{-3}$. These estimates pertain only to the observed medium at $T \sim 10^4$ K. The cloud could be ionized and heated by the active nucleus of the galaxy, since the nebula apparently intercepts enough of the ultraviolet radiation from the nucleus to explain the observed $H\alpha$ luminosity, even if the gas is optically thin to the Lyman continuum. Assuming that the radiating material is ejecta from the nucleus, we then estimate a travel time for the nucleus of $\sim 10^6$ years, that the nebular mass $\sim 10^6 M_\odot$ ($n_e \sim 200 \text{ cm}^{-3}$), and that nebular confinement by the ram pressure of the galaxy's halo is possible. We thus obtain a kinetic energy of $\sim 10^{56}$ ergs in the emitting gas. This model does not address some aspects of the nebula, but further observations are required before more sophisticated modeling can be attempted.

We wish to thank Dr. Harvey Butcher and the KPNO staff for ably assisting us through the observations. T. H. was partially supported by NATO Research grant (1828), and B. B. by funds generously provided by the Graduate Student Research Fund of the University of Washington and the Research Corporation. T. H. wishes to express appreciation to the staff of Sterrewacht Leiden for nearly two years of hospitality during which this work was conducted. Ray Weymann, John Scott, and Dave Turnshek are thanked for interesting conversations about the possible relevance of the broad absorption lines seen in quasars to the Mrk 335 phenomenon.

REFERENCES

- Adams, T. F. 1977, *App. J. Suppl.*, **33**, 19.
 Baldwin, J. A., Carswell, R. F., Wampler, E. J., Smith, H. E., Burbidge, E. M., and Boksenberg, A. 1980, *Ap. J.*, **236**, 388.
 Balick, B., and Heckman, T. M. 1979, *A.J.*, **84**, 302.
 Bregman, J. N. 1980, *Ap. J.*, **237**, 681.
 Capriotti, E., Foltz, C., and Byard, P. 1979, *Ap. J.*, **230**, 681.
 de Bruyn, A. G., and Sargent, W. L. W. 1978, *A.J.*, **83**, 1257.
 Dower, R. G., Griffiths, R. E., Bradt, H. V., Doxsey, R. E., and Johnson, M. D. 1980, *Ap. J.*, **235**, 355.
 Ferland, G. J., Netzer, H., and Shields, G. A. 1979, *Ap. J.*, **232**, 382.
 Margon, B., Chanan, G. A., and Romanishin, W. 1981, *Ap. J. (Letters)*, in press.
 Miley, G. K. 1980, *Ann. Rev. Astr. Ap.*, **18**, 165.
 Norman, C., and Silk, J. 1979, *Ap. J. (Letters)*, **233**, L1.
 Oke, J. B. 1974, *Ap. J. Suppl.*, **27**, 21.
 Osterbrock, D. E. 1977, *Ap. J.*, **215**, 753.
 ———, 1979, *A.J.*, **84**, 901.
 Phillips, M. M. 1977, *Ap. J.*, **215**, 746.
 Rieke, G. H. 1978, *Ap. J.*, **226**, 550.
 Robinson, W., Ball, W., Vokac, P., Piegorsch, W., and Reed, R. 1979, *Proc. SPIE Symposium, Instrumentation in Astronomy*, No. 3, **172**, 98.
 Sandage, A. R., and Visvanathan, N. 1978, *Ap. J.*, **223**, 707.
 Turnshek, D. A., Weymann, R. J., Liebert, J. W., Williams, R. E., and Strittmatter, P. A. 1980, *Ap. J.*, **238**, 488.
 Ulrich, M. H., and Péquinot, D. 1980, *Ap. J.*, **238**, 45.
 Weedman, D. W., 1977, *Ann. Rev. Astr. Ap.*, **15**, 69.

B. BALICK: Department of Astronomy, University of Washington, Seattle, WA 98195

T. M. HECKMAN: Steward Observatory, University of Arizona, Tucson, AZ 85721